Int J Coal Sci Technol (2014) 1(3):315–320
DOI 10.1007/s40789-014-0037-y

Conversion of producer gas using NiO/SBA-15 obtained with different synthesis methods

Baowang Lu · Yiwen Ju · Katsuya Kawamoto

Received: 25 October 2013 / Revised: 20 December 2013 / Accepted: 2 January 2014 / Published online: 18 October 2014
© The Author(s) 2014. This article is published with open access at Springerlink.com

Abstract In this study, NiO/SBA-15 was prepared by both direct and post synthesis methods. TEM images revealed that NiO particles aggregated in NiO/SBA-15 obtained with post synthesis method, regardless of NiO loading. However, NiO particles were monodispersed in NiO/SBA-15 with a NiO loading of less than 15 wt% by using the direct synthesis method. In this case, NiO particles aggregated when NiO loading was over 20 wt%. TPR analysis verified that with direct synthesis method the location boundary of NiO particles on outer and pore surface could be observed clearly, whereas that could not observed in the case of post synthesis method. This indicates that the type of synthesis method displays significant effect on the location of NiO particles dispersed into the SBA-15. Producer gas conversion was carried out using NiO/SBA-15 as catalysts, which were synthesized with different synthesis methods. The gas conversion including methanation occurred at low temperature (i.e., 300–400 °C) and the reverse water gas shift (RWGS) reaction at high temperature (i.e., 400–900 °C). High temperatures facilitated CO_2 conversion to CO with CO selectivity close to 100 %, regardless of the synthesis method of the used catalyst. At low temperatures the dispersion type of NiO particles affected the CO_2 conversion reaction, i.e., monodispersed NiO particles gave a CO selectivity of close to 100 %, similar to that obtained at high temperature. The aggregated NiO particles resulted in a CO selectivity of less than 100 % owing to CH_4 formation, regardless of synthesis method of catalyst. Therefore, NiO/SBA-15 obtained with direct synthesis method favored RWGS reaction because of high CO selectivity. NiO/SBA-15 obtained with post synthesis method is suited for methanation because of high CH_4 selectivity, and the conversion of CO_2 to CH_4 through methanation increased with increasing NiO loading.

Keywords Nickel · Mesoporous silica · Synthesis method · Producer gas · Methanation · Reverse water gas shift (RWGS) reaction

B. Lu (✉)
Center for Material Cycles and Waste Management Research, National Institute for Environmental Studies, 16-2 Onogawa, Tsukuba, Ibaraki 305-8506, Japan
e-mail: lu.baowang@nies.go.jp

Y. Ju
Laboratory of Computational Geodynamics College of Earth Science, University of Chinese Academy of Sciences, Beijing 100049, China

K. Kawamoto
Graduate School of Environmental Science, Okayama University, 3-1-1 Tsushima-naka, Kita-ku, Okayama-shi, Okayama 700-8530, Japan

1 Introduction

As an important energy resource for replacing petroleum, coal and biomass have attracted great interest. Gasification is an important process as regards to the utilization of them in energy recycling, namely, converting into a producer gas mixture consisting of carbon monoxide (CO), hydrogen (H_2), carbon dioxide (CO_2) and other trace species (Huber et al. 2006; Zhu et al. 2008; Yung et al. 2009). As the gas mixture has a low energy density, its utilization value is very low. To increase the energy density or calorific value, the producer gas is often reformed to produce useable H_2 (Antal et al. 2000; Lee et al. 2002; Hao et al. 2003, 2005;

Sınag et al. 2003; Lu et al. 2006; Byrd et al. 2007), CO (Ashcroft et al. 1991; Fox 1993; Rostrup-Nielsen and Bak-Hansen 1993) and synthetic natural gas (SNG) (Seemann et al. 2006, 2010; Kopyscinski et al. 2009, 2010). Because CO_2 is the most difficult producer gas to convert, its conversion remains an important topic.

The conversion of CO_2 to valuable chemical materials has been proposed as a possible way of utilizing non-combustible CO_2 (Jessop et al. 2004; Sakakura et al. 2007; Centi and Perathoner 2009; Federsel et al. 2010; Mikkelsen et al. 2010; Bourrez et al. 2011). In terms of CO_2 conversion, since CO is a valuable material in many chemical processes, the conversion of CO_2 to CO through the reverse water gas shift (RWGS) reaction by catalytic hydrogenation is recognized as the most promising process. In addition, CO_2 methanation is also an important process, and has been investigated for the production of energy carriers (Weatherbee and Bartholomew 1981; Peebles et al. 1983; Yamasaki et al. 2006; Ocampo et al. 2009), since this reaction is considerably faster than other reactions that form hydrocarbons or alcohols (Inu and Takeguchi 1991).

Nickel(Ni)-based catalysts remain the most extensively studied well-dispersed materials, and Ni-based catalysts have been investigated for the RWGS reaction and methanation (Vance and Bartholomew 1983; Wang et al. 2008). The discovery of ordered mesostructured silica SBA-15 with an adjustable pore size and a high specific surface area (Zhao et al. 1998, 2014) has provided the opportunity to produce well-dispersed Ni catalysts. NiO/SBA-15 has been realized with a post synthesis method (Vradman et al. 2005; Cheng et al. 2009; Lu and Kawamoto 2012), and methanation has been investigated (Lu and Kawamoto 2013). In addition, highly loaded and well-dispersed NiO/SBA-15 has been obtained by the direct synthesis method for the first time (Lu and Kawamoto 2012). However, the differences in location and dispersion of NiO particles caused by synthesis method in SBA-15 are not yet clear.

Therefore, we synthesized NiO/SBA-15 with 10 wt% NiO using direct and post synthesis methods, respectively. Their TEM observations were carried out to investigate the dispersion of NiO particles in SBA-15. H_2-TPR was used to study the location and dispersion of NiO particles in SBA-15. The RWGS reaction and methanation were carried out using NiO/SBA-15 obtained with different synthesis methods and NiO loadings.

2 Experimental

According to the previous report (Lu and Kawamoto 2012), the direct synthesis method was used to prepare NiO/SBA-15. The block copolymer Pluronic P123 was mixed with water, H_2SO_4, $Ni(NO_3)_2{\cdot}6H_2O$, and tetraethyl orthosilicate at room temperature. The mixture was aged at 60 °C until a white precipitate appeared and then immediately evaporated at 100 °C overnight. The solid product was dried at 150 °C for 5 h and then calcined at 500 °C for 10 h then 800 °C for 2 h.

With post synthesis method, SBA-15 was firstly synthesized at 60 °C according to the method (Chen et al. 2003). Then as described in the literature (Lu and Kawamoto 2013), the SBA-15 was added to EtOH containing dissolved $Ni(NO_3)_2{\cdot}6H_2O$ and dispersed for 6 h under supersonic. The mixture was then dried at room temperature and calcined at 400 °C for 5 h. The solid products were characterized by TEM observation. The catalyst reducibility was also studied by temperature programmed reduction (TPR) in BET-CAT catalyst analyzer (BEL Japan Inc.) using H_2.

The RWGS reaction and methanation were performed as follows. The catalysts were pre-reduced before the reaction. The reaction was performed at atmospheric pressure in a fixed-bed quartz reactor. A 30-mm long catalyst (2 g) between two layers of quartz wool was loaded into the reactor. The reactor was heated in a furnace. All reactant gases were monitored by mass flow meter and controller. The flow of the product was measured with a film flow meter and analyzed by GC-TCD after the reaction had become stable.

3 Results and discussion

As shown in Fig. 1a, the small-angle XRD patterns of NiO/SBA-15 with NiO loading of 10 wt% had three well-resolved peaks, indicative of the typical two-dimensional hexagonally ordered mesostructure of SBA-15, regardless of the synthesis method. However, the angles of all of the diffraction peaks of NiO/SBA-15 obtained with direct synthesis method were smaller than those obtained with post synthesis method. This result suggests that the pore size of SBA-15 differed with synthesis method—in other words, the synthesis method affected the pore size of SBA-15. With post synthesis method, the NiO particles were inserted into the SBA-15 pores, resulting in the decrease of pore size. The wide-angle XRD peaks could be indexed to a face-centered cubic crystalline NiO structure, irrespective of synthesis method (Fig. 1b), indicating that NiO particles were also dispersed on the outer surface besides on pore surface of SBA-15. All wide-angle peak intensities of NiO/SBA-15 obtained with direct synthesis method were greater than those with post synthesis method. This result suggests that, with direct synthesis method, the NiO amount located on outer surface of NiO/SBA-15 was high. In addition, a broad peak at around $2\theta = 23°$ caused by the amorphous

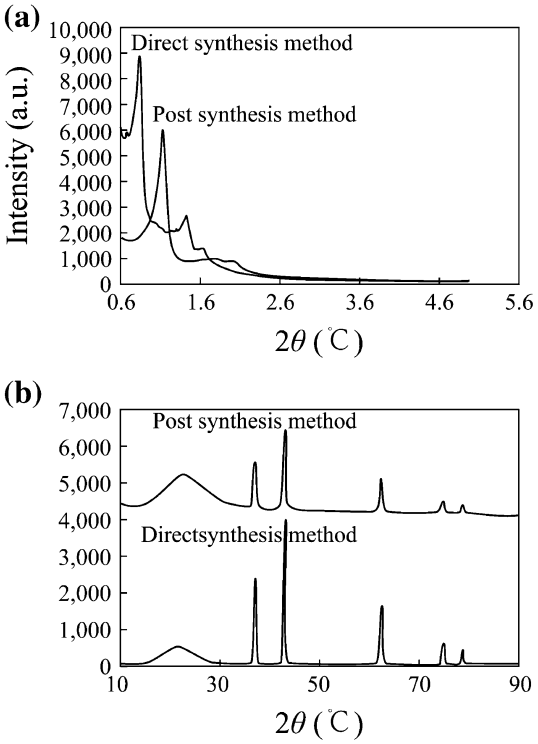

Fig. 1 XRD patterns of 10 wt% NiO/SBA-15

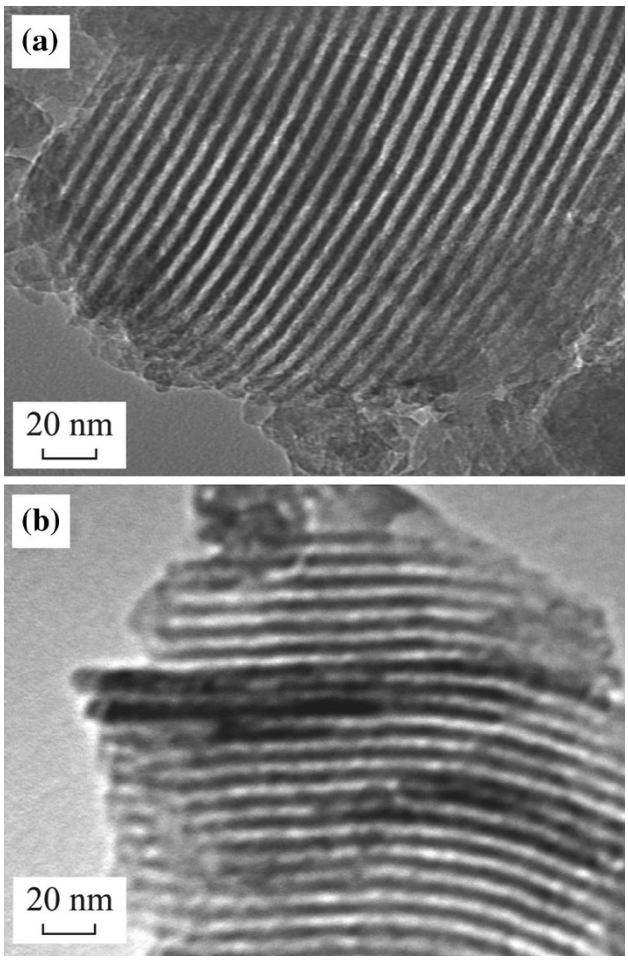

Fig. 2 TEM images of NiO/SBA-15 obtained by direct synthesis and post-synthesis methods

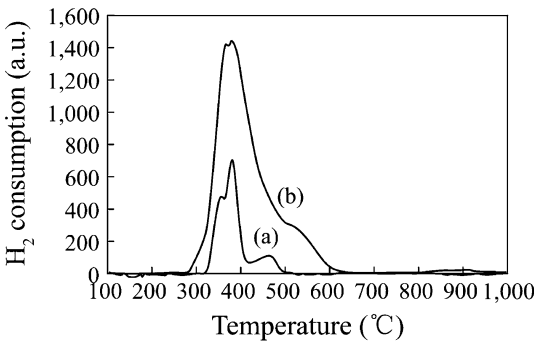

Fig. 3 H_2-TPR profiles of NiO/SBA-15 obtained by direct synthesis and post synthesis methods

SiO_2 structure of SBA-15 was clearly observed in the wide-angle XRD pattern, indicating that the ordered mesoporous SBA-15 structure was not disturbed by the included NiO.

We examined the nitrogen adsorption–desorption isotherms of NiO/SBA-15 with NiO loading of 10 wt% obtained by using two different synthesis methods (not shown). The isotherms were similar to the type IV IUPAC classification, clearly indicating that these materials possessed mesoporous structures, and a type-H1 hysteresis loop was observed, regardless of synthesis method. The isotherms were typical of SBA-15, indicating the formation of a p6mm structure with open cylindrical mesopores. It was very clear that the decrease of pore size was caused by NiO particles included through post synthesis method.

The TEM images of NiO/SBA-15 with NiO loading of 10 wt% showed an ordered mesoporous structure typical of SBA-15, irrespective of synthesis method (Fig. 2a, b). With direct synthesis method (Fig. 2a), NiO particles were highly dispersed (monodispersed) into the SiO_2 structure of SBA-15. With post-synthesis method, aggregates of NiO particles were observed clearly (Fig. 2b).

TPR investigation is generally useful as a fingerprint of a metal species' interaction with the support material. As shown in Fig. 3a, for NiO/SBA-15 obtained with direct synthesis method, H_2-TPR profiles exhibited three sharp peaks. The former two peaks were ascribed to NiO particles on the outer surface of SBA-15, while the last peak was assigned to those on the pore surface of SBA-15, indicating that NiO particles were highly and well-dispersed into SBA-15, and the located boundary of NiO particles on between pore and outer surface could be observed. However, for NiO/SBA-15 obtained with post

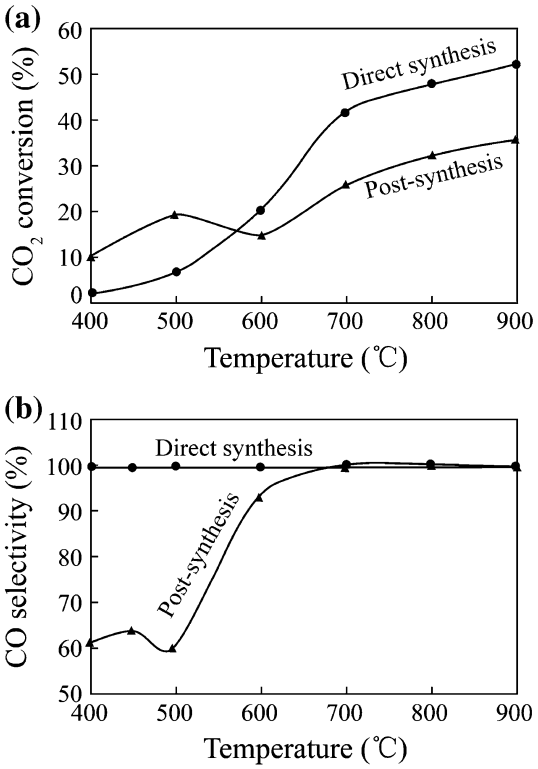

Fig. 4 CO_2 conversion and CO selectivity with different 10 wt% NiO/SBA-15 obtained by the direct synthesis and post-synthesis methods. *Notes* CO_2:H_2 = 60:60 mL/min

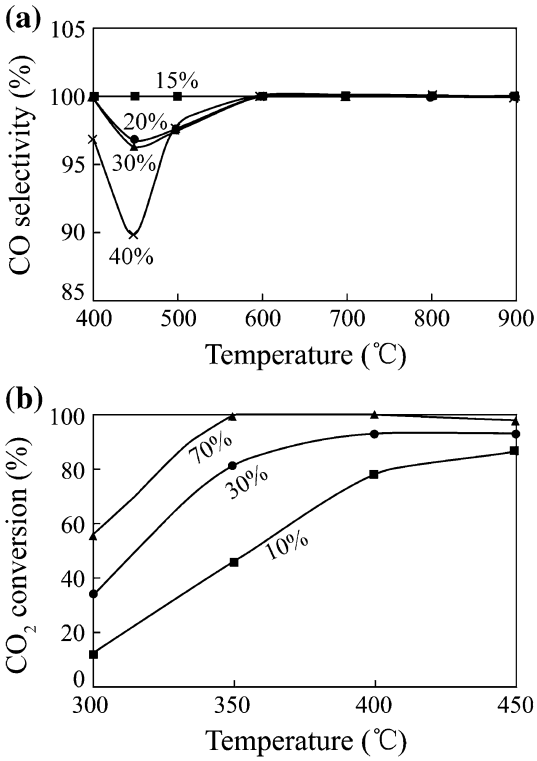

Fig. 5 CO selectivity using NiO/SBA-15 obtained by the direct synthesis method with different NiO loadings and CO_2 conversion using NiO/SBA-15 obtained by the post-synthesis method with different NiO loadings. *Notes* CO_2:H_2 = 30:210 mL/min

synthesis method (Fig. 3b), H_2-TPR profiles exhibited only a broad peak centered at 378 °C, indicating that NiO particles located either in pore or on outer surface could be observed, but their location boundary could not be distinguished clearly. Therefore, with post synthesis method, NiO particles were more poorly dispersed (aggregated) in SBA-15 than that with direct synthesis method.

We used 10 wt% NiO/SBA-15 obtained by direct synthesis and post-synthesis methods to investigate the RWGS reaction (Fig. 4). When NiO/SBA-15 obtained by direct synthesis method was used, CO_2 conversion increased with increasing temperature (Fig. 4a). Using NiO/SBA-15 obtained by post synthesis method, CO_2 conversion increased with increasing temperature at temperatures of 600 °C or above; however, the CO_2 conversion efficiency was lower than that obtained using NiO/SBA-15 synthesized by direct synthesis method. At low temperatures (lower than 500 °C), because CO_2 methanation occurred, the CO_2 conversion percentage was higher than that obtained using NiO/SBA-15 synthesized by direct synthesis method. Therefore, NiO/SBA-15 obtained by direct synthesis method favoured the RWGS reaction, but that obtained by post synthesis method catalyzed both RWGS reaction (by-reaction) and methanation (main reaction), which suited for methanation. Using NiO/SBA-15 obtained by direct synthesis method, the CO selectivity was 100 %, regardless of the temperature (Fig. 4b). Using NiO/SBA-15 obtained by post synthesis method, the CO selectivity was 100 % at temperatures of 700 °C and above. But at lower temperatures it was not 100 %, owing to the formation of CH_4. Therefore, CO selectivity seems to be affected by synthesis method. However, based on the above TEM observations, we found that the dispersion of NiO particles, instead of synthesis method, affected the selectivity to CO.

We varied the NiO loading to investigate the RWGS reaction using NiO/SBA-15 obtained by direct synthesis method. CO_2 conversion increased with increasing temperature, regardless of the NiO loading, which is far higher than conventional Cu catalysts (Chen et al. 2003, 2004). When the NiO loading was less than 15 wt%, the CO selectivity was close to 100 %, regardless of temperature. This indicates that NiO particles were monodispersed when the NiO loading exceeded 20 wt%, and the CO selectivity was 100 % at temperatures of 600 °C or above, regardless of the NiO loading (Fig. 5a). However, at temperatures below 600 °C the CO selectivity was lower than 100 %, owing to the formation of CH_4, indicating NiO particles aggregated. Therefore, CO selectivity was influenced by NiO loading at low temperatures. To obtain CO with a

selectivity of 100 %, the RWGS reaction should therefore be performed at an appropriate temperature and using NiO/SBA-15 with an appropriate NiO loading (NiO dispersion) as a catalyst.

Finally, methanation was performed with NiO/SBA-15 obtained by post synthesis method and with different NiO loadings. CO_2 conversion increased with increasing NiO loading (Fig. 5b). When 70 wt% NiO/SBA-15 was employed, CO_2 conversion of 99.2 % was achieved. These values are the highest yet reported comparison with the previous report (Perkas et al. 2009). The value was still 89.4 % at an H_2 to CO_2 ratio of 4:1. These values are the highest yet reported. The CH_4 selectivity was 100 % when the NiO amount exceeded 50 wt%, regardless of the NiO/SBA-15 preparation method; in other words, release of CO as a by-product was completely suppressed.

4 Conclusions

Novel NiO/SBA-15 catalysts were obtained with different synthesis methods for producer gas conversion. The synthesis method affected the location and dispersion of NiO particles in SBA/15. High temperature facilitated RWGS reaction, regardless of synthesis method. At low temperature, CO_2 conversion reaction was dependent on synthesis method. With direct synthesis method, NiO loading affected CO selectivity only at low temperatures owing to CH_4 formation. With post synthesis method, CO_2 conversion to CH_4 through methanation increased with increasing NiO loading.

Open Access This article is distributed under the terms of the Creative Commons Attribution License which permits any use, distribution, and reproduction in any medium, provided the original author(s) and the source are credited.

References

Antal MJ, Allen SG, Schulman D, Xu XD, Divilio RJ (2000) Biomass gasification in supercritical water. Ind Eng Chem Res 39(11):4040–4053

Ashcroft AT, Cheetham AK, Green MLH, Vernon PDF (1991) Partial oxidation of methane to synthesis gas using carbon dioxide. Nature 352(6332):225–226

Bourrez M, Molton F, Chardon-Noblat S, Deronzier A (2011) [Mn(bipyridyl)(CO)3Br]: an abundant metal carbonyl complex as efficient electrocatalyst for CO2 reduction. Angew Chem Int Ed 50(42):9903–9906

Byrd AJ, Pant KK, Gupta RB (2007) Hydrogen production from glucose using Ru/Al2O3 catalyst in supercritical water. Ind Eng Chem Res 46(11):3574–3579

Centi G, Perathoner S (2009) Opportunities ad prospects in the chemical recycling of carbon dioxide to fuels. Catal Today 148:191–205

Chen CS, Cheng WH, Lin SS (2003) Study of reverse water gas shift reaction by TPD, TPR and CO2 hydrogenation over potassium-promoted Cu/SiO2 catalyst. Appl Catal A 238(1):55–67

Chen CS, Cheng WH, Lin SS (2004) Study of iron-promoted Cu/SiO2 catalyst on high temperature reverse water gas shift reaction. Appl Catal A 257(1):97–106

Cheng MY, Pan CJ, Hwang BJ (2009) Highly-dispersed and thermally-stable NiO nanoparticles exclusively confined in SBA-15: blockage-free nanochannels. J Mater Chem 19(29):5193–5200

Federsel C, Jackstell R, Beller M (2010) State-of-the-art catalysts for hydrogenation of carbon dioxide. Angew Chem Int Ed 49(36):6254–6257

Fox JM III (1993) The different catalytic routes for methane valorization: an assessment of processes for liquid fuels. Catal Rev Sci Eng 35:169–212

Hao XH, Guo LJ, Mao X, Zhang XM, Chen XJ (2003) Hydrogen production from glucose used as a model compound of biomass gasified in supercritical water. Int J Hydrog Energy 28(1):55–64

Hao XH, Guo LJ, Zhang XM, Guan Y (2005) Hydrogen production from catalytic gasification of cellulose in supercritical water. Chem Eng J 110(1–3):57–65

Huber GW, Iborra S, Corma A (2006) Synthesis of transportation fuels from biomass: chemistry, catalysts, and engineering. Chem Rev 106(9):4044–4098

Inu T, Takeguchi T (1991) Effective conversion of carbon dioxide and hydrogen to hydrocarbons. Catal Today 10:95–106

Jessop PG, Joo F, Tai CC (2004) Recent advances in the homogeneous hydrogenation of carbon dioxide. Coord Chem Rev 248(21–24):2425–2442

Kopyscinski J, Schildhauer TJ, Biollaz SMA (2009) Employing catalyst fluidization to enable carbon management in the synthetic natural gas production from biomass. Chem Eng Technol 32(3):343–347

Kopyscinski J, Schildhauer TJ, Biollaz SMA (2010) Production of synthetic natural gas (SNG) from coal and dry biomass: a technology review from 1950 to 2009. Fuel 89(8):1763–1783

Lee IG, Kim MS, Ihm SK (2002) Gasification of glucose in supercritical water. Ind Eng Chem Res 41(5):1182–1188

Lu BW, Kawamoto K (2012) Direct synthesis of highly loaded and well-dispersed NiO/SBA-15 for producer gas conversion. RSC Adv 2(17):6800–6805

Lu BW, Kawamoto K (2013) Preparation of the highly loaded and well-dispersed NiO/SBA-15 for methanation of producer gas. Fuel 103:699–704

Lu YJ, Guo LJ, Ji CM, Zhang XM, Hao XH, Yan QH (2006) Hydrogen production by biomass gasification in supercritical water: a parametric study. Int J Hydrog Energy 31(7):822–831

Mikkelsen M, Jorgensen M, Krebs FC (2010) The teraton challenge: a review of fixation and transformation of carbon dioxide. Energy Environ Sci 3(1):43–81

Ocampo F, Louis B, Roger AC (2009) Methanation of carbon dioxide over nickel-based Ce0.72Zr0.28O2 mixed oxide catalysts prepared by sol–gel method. Appl Catal A General 369(1-2):90–96

Peebles DE, Goodman JM, White JM (1983) Methanation of carbon dioxide on Ni(100) and the effects of surface modifiers. J Phys Chem 87:4378–4387

Perkas N, Amirian G, Zhong ZY, Teo J, Gofer Y, Gedanken A (2009) Methanation of carbon dioxide on Ni catalysts on mesoporous ZrO2 doped with rare earth oxides. Catal Lett 130(3–4):455–462

Rostrup-Nielsen JR, Bak-Hansen JH (1993) CO_2-reforming of methane over transition metals. J Catal 144:38–49

Sakakura T, Choi JC, Yasuda H (2007) Transformation of carbon dioxide. Chem Rev 107(6):2365–2387

Seemann MC, Schildhauer TJ, Biollaz SMA, Stucki S, Wokaun A (2006) The regenerative effect of catalyst fluidization under methanation conditions. Appl Catal A General 313(1):14–21

Seemann MC, Schildhauer TJ, Biollaz SMA (2010) Fluidized bed methanation of wood-derived producer gas for the production of synthetic natural gas. Ind Eng Chem Res 49:7034–7038

Sınag A, Kruse A, Schwarzkopf V (2003) Key Compounds of the hydropyrolysis of glucose in supercritical water in the presence of K_2CO_3. Ind Eng Chem Res 42:3516–3521

Vance CK, Bartholomew CH (1983) Hydrogenation of carbon dioxide on group VIII materials. III, Effects of support on activity/selectivity and adsorption properties of nickel. Appl Catal 7:169–177

Vradman L, Landau MV, Kantorovich D, Koltypin Y, Gedanken A (2005) Evaluation of metal oxide phase assembling mode inside the nanotubular pores of mesostructured silica. Microporous Mesoporous Mater 79(1–3):307–318

Wang L, Zhang S, Liu Y (2008) Reverse water gas shift reaction over Co-precipitated Ni-CeO2 catalysts. J Rare Earths 26:66–70

Weatherbee GD, Bartholomew CH (1981) Hydrogenation of CO2 on group VIII metals: I. specific activity of Ni/SiO2. J Catal 68:67–76

Yamasaki M, Habazaki H, Asami K, Izumiya K, Hashimoto K (2006) Effect of tetragonal ZrO on the catalytic activity of Ni/ZrO catalyst prepared from amorphous Ni–Zr alloys. Catal Commun 7:24–28

Yung MM, Jablonski WS, Magrini-Bair KA (2009) Review of catalytic conditioning of biomass-derived syngas. Energy Fuels 23:1874–1883

Zhao D, Feng J, Huo Q, Melosh N, Fredrickson GH, Chmelka BF, Stuchy GD (1998) Triblock copolymer syntheses of mesoporous silica with periodic 50 to 300 angstrom pores. Science 279:548–552

Zhao DY, Huo QS, Feng JL, Chmelka BF, Stucky GD (2014) Correction to "nonionic triblock and star diblock copolymer and oligomeric surfactant syntheses of highly ordered, hydrothermally stable, mesoporous silica structures". J Am Chem Soc 136(29):10546

Zhu WK, Song WL, Lin WG (2008) Catalytic gasification of char from co-pyrolysis of coal and biomass. Fuel Process Technol 89(9):890–896